Available online at www.sciencedirect.com
ScienceDirect
Polymer 49 (2008) 554–560
polymer
www.elsevier.com/locate/polymer

# Fluorescence spectra of poly(di-*n*-hexylsilane)/$TiO_2$ nanoparticle hybrid film

Akira Watanabe [a,*], Tokuji Miyashita [a], Atsuo Kasuya [b], Masae Takahashi [c], Yoshiyuki Kawazoe [c]

[a] *Institute of Multidisciplinary Research for Advanced Materials, Tohoku University, Sendai 980-8577, Japan*
[b] *Center for Interdisciplinary Research, Tohoku University, Sendai 980-8578, Japan*
[c] *Institute for Materials Research, Tohoku University, Sendai 980-8577, Japan*

Received 3 August 2007; received in revised form 11 November 2007; accepted 17 November 2007
Available online 3 December 2007

**Abstract**

The interaction between poly(di-*n*-hexylsilane) (PDHS) and $TiO_2$ nanoparticle was studied based on the temperature dependence of the fluorescence of a PDHS/$TiO_2$ nanoparticle hybrid film. The polysilane is a suitable probe to investigate a guest polymer–host matrix interaction because the photophysical properties of polysilanes remarkably depend on the conformation of the σ-conjugated Si–Si chain. The PDHS/$TiO_2$ nanoparticle hybrid film showed a fluorescence band assigned to a disordered structure even at 80 K whereas only the fluorescence band of an ordered structure was observed for the PDHS film at 80 K. The disordering of the Si–Si main chain was explained by the perturbation of the *n*-hexyl side chain in the neighborhood of the $TiO_2$ nanosurface. The non-radiative deactivation of the excited state via the disorder-induced local potential minima was suggested by the temperature dependence of the fluorescence intensities of the disordered and ordered structures in the temperature region from 80 to 160 K.


*Keywords:* Polysilane; $TiO_2$ nanoparticle; Fluorescence

## 1. Introduction

Polysilanes are organosilicon polymers consisting of a Si–Si main chain and organic side chains (Fig. 1). The linear Si–Si chain of a polysilane can be considered to be a pseudo-one-dimensional silicon chain. The polysilanes show unique properties due to the σ-conjugation along the Si–Si main chain [1–13]. The photophysical properties of the polysilanes are quite sensitive to the polymer conformation because the electronic state is strongly dominated by the overlapping of the σ-conjugated electron along the Si–Si main chain. The absorption and fluorescence spectra of the polysilanes show thermochromism due to the order–disorder transition of the polymer backbone conformation. An all-*trans* (planar zigzag) conformation has been proposed as an ordered structure of the poly(di-*n*-hexylsilane) (PDHS) in the solid state [1,6].

With increasing the temperature, the PDHS shows the order–disorder transition at around 42 °C, where the main chain changes from a *trans*-rich to a *gauche*-rich conformation [2]. The structure of the alkyl-substituted polysilane in a high-temperature phase has been described as columnar liquid crystalline with hexagonal symmetry [1,3,4].

The conformation of PDHS is sensitive to the environment. In previous papers, we have reported the fluorescence spectra of the PDHS incorporated into a nanoporous silica material as a host matrix [14–18]. The pore size and the chemical structure of the pore surface remarkably influence the fluorescent properties. It has been demonstrated that the fluorescent properties are significantly different from the PDHS due to both polymer–polymer and polymer–surface interaction in the nanopore. The polysilane chains near the pore boundaries and in the pore center evidently should have different

* Corresponding author. Tel./fax: +81 22 217 5659.
*E-mail address:* watanabe@tagen.tohoku.ac.jp (A. Watanabe).

0032-3861/$ - see front matter © 2007 Elsevier Ltd. All rights reserved.
doi:10.1016/j.polymer.2007.11.052

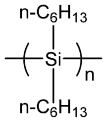


Fig. 1. Chemical structure of poly(di-*n*-hexylsilane).

properties, where the polymer–surface interaction leads to the *gauche* conformation. The polysilane is a suitable probe to investigate the guest polymer–host matrix interaction because the photophysical properties of the polysilane remarkably depend on the conformation of the σ-conjugated Si–Si chain.

Recently, semiconducting polymer/nanoporous $TiO_2$ heterojunction solar cells have been reported [19–24]. Although such photovoltaic devices are promising candidates due to the synthetic flexibility and the manufacturing advantage, up to now none of the efforts have led to a power conversion efficiency above 1% for the solar cell using $TiO_2$/semiconducting polymer heterojunction. In comparison with silicon solar cell, the properties of the space charge layer of the $TiO_2$/semiconducting polymer are very complicated as a result of the heterojunction between the nanoporous $TiO_2$ and the semiconducting polymer chain. The conversion efficiency of the device depends on the manufacturing process of the cell because the understanding of the natures of polymers in nanostructured materials has not been enough. It is important to accumulate fundamental data on the properties of the interface between the nanostructured $TiO_2$ and the semiconducting polymers. In this paper, we studied the PDHS/$TiO_2$ nanoparticle hybrid film using the fluorescence of the PDHS as a probe to elucidate the interaction between the polymer chain and the $TiO_2$ nanoparticle.

## 2. Experimental

### 2.1. Materials

The PDHS was synthesized by Wurtz-type reaction of di-*n*-hexyldichlorosilane using a sodium metal in toluene at 110 °C with rapid stirring. The molecular weight, $M_w$, and the distribution ($M_w/M_n$, $M_w$: weight-average molecular weight; $M_n$: number-average molecular weight) of the PDHS were determined to be 21,000 and 1.19, respectively, by gel permeation chromatography (GPC) using tetrahydrofuran (THF) as the eluent and monodispersed polystyrenes as the standards. A $TiO_2$ nanoparticle was purchased from TAYCA Co. (TK-294, colloidal anatase nanoparticle size about 20 nm) as a $TiO_2$ paste dispersed in a water phase. The dispersion medium was exchanged from the water to dimethylformamide (DMF) by centrifugal separation method. The dispersion medium was exchanged again from the DMF to toluene by centrifugal separation method just before mixing with the PDHS. After mixing the PDHS and the $TiO_2$ nanoparticle in toluene, the mixture was ultrasonicated for 10 min. The weight percentages of the PDHS and the $TiO_2$ nanoparticle in the solution were 2% and 10%, respectively. The PDHS/$TiO_2$ nanoparticle paste was coated on a quartz substrate by doctor blading technique with a Scotch tape as frame and spacer, raking off the excess paste with a glass rod. The thickness of the PDHS/$TiO_2$ nanoparticle film on a quartz substrate was ca. 50 μm after vacuum drying.

### 2.2. Measurements

The differential scanning calorimetry (DSC) was carried out by DSC-60 (Shimadzu) under He atmosphere. The samples were placed in a cryostat (JANIS, VPF-475) equipped with a temperature controller (LakeShore, Model 330). The cryostat was evacuated below ca. $10^{-3}$ Pa by a turbo-molecular pump. The samples were cooled by liquid $N_2$ in the cryostat before measurements. The excitation source was the 325 nm line of a He–Cd laser (KIMMON KOHACO., LTD, IK5751I-G). The fluorescence spectra were measured by a CCD camera (DV401, Andor Technology) attached to a monochromator (MS257, Oriel Instruments Co.).

## 3. Results and discussion

### 3.1. Fluorescence of the PDHS/$TiO_2$ nanoparticle hybrid film

A complicated temperature dependence was observed in the fluorescence spectra of the PDHS/$TiO_2$ nanoparticle hybrid film. Fig. 2 shows the fluorescence spectra of the PDHS/$TiO_2$ nanoparticle hybrid film at 80, 260, 315, and 320 K, where the intensities are normalized at each peak.

The fluorescence spectrum of the PDHS/$TiO_2$ nanoparticle hybrid film at 80 K shows 355 and 371 nm peaks, which can be assigned to the disorder and order structures of the Si–Si main chain, respectively. It is unusual for the PDHS to show the disordered structure below room temperature. As shown in Fig. 2a, the disordered structure was observed even at 80 K. The 355-nm band disappeared at around 260 K accompanying the shift of the fluorescence peak of the ordered structure toward longer wavelengths (Fig. 2b). With increasing the temperature up to 315 K, the fluorescence peak assigned to the

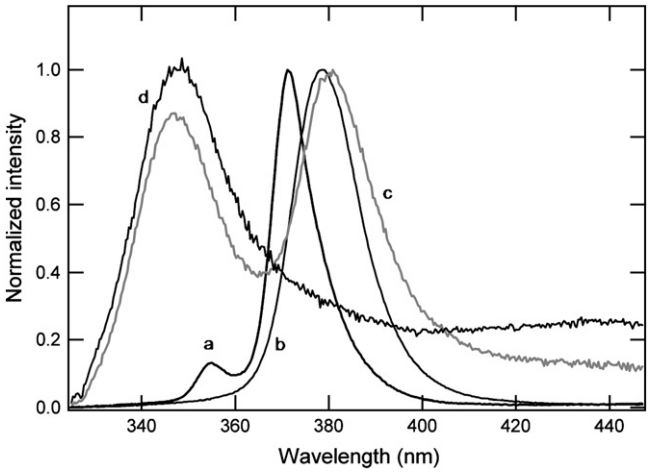


Fig. 2. Fluorescence spectra of the PDHS/$TiO_2$ nanoparticle hybrid film at various temperatures: (a) 80, (b) 260, (c) 315, (d) 320 K. The intensities are normalized at each peak.

disordered structure appeared again at 347 nm (Fig. 2c, d). In the following, we compared the temperature dependence of the fluorescence spectra of the PDHS and the PDHS/$TiO_2$ nanoparticle hybrid film in detail.

### *3.2. Temperature dependence of the fluorescence of the PDHS film*

The temperature dependence of fluorescence of the PDHS film in the region from 80 to 260 K is shown in Fig. 3.

The fluorescence spectrum at 80 K shows the maximum at 374 nm, which is assigned to the ordered structure. The fluorescence intensity decreases with increasing temperature due to the increase of the non-radiative deactivation processes. Another noticeable feature is the shift of the fluorescence maximum to longer wavelengths with increasing temperature. The maximum wavelength shifts from 374 nm at 80 K to 380 nm at 260 K. On the other hand, the fluorescence maximum is almost constant at around 380 nm in the temperature region from 260 to 315 K as shown in Fig. 4. The fluorescence spectrum at 315 K exhibits a weak band at 347 nm. In Fig. 5, the fluorescence band at 380 nm disappears at 320 K and the spectrum shows only the 347-nm band above 320 K. Such a spectral change from 380 to 347 nm band has been assigned to the order–disorder transition where the *trans*-rich conformation of the Si–Si main chain changes into the *gauche*-rich conformation.

The temperature dependence of the absorption spectrum gives some powerful supports on the backbone structures around the order–disorder transition temperature. Fig. 6 shows temperature dependence of the absorption spectrum of the PDHS film around the order–disorder transition temperature, where the absorption peaks at around 360 and 310 nm are assigned to those of ordered and disordered structures, respectively. The transition temperature of the order–disorder transition is also observed at around 315 K.

The image of the conformational transition is illustrated schematically in Fig. 7. Molecular models of (a) and (b) show the all-*trans* (planar zigzag) and the disordered

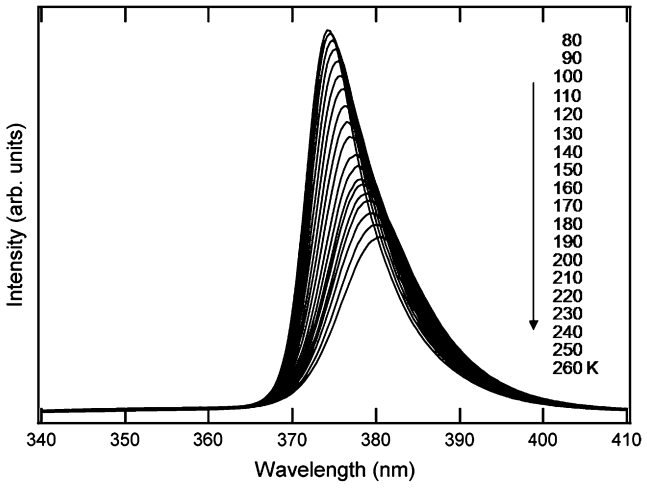


Fig. 3. Fluorescence spectra of the PDHS film in the temperature region from 80 to 260 K.

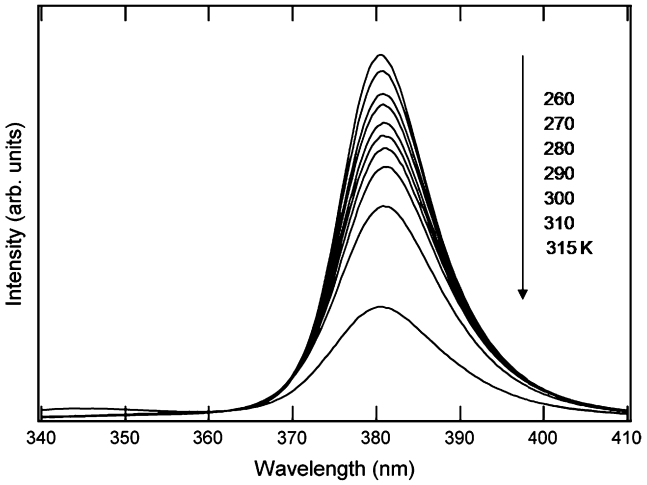


Fig. 4. Fluorescence spectra of the PDHS film in the temperature region from 260 to 315 K.

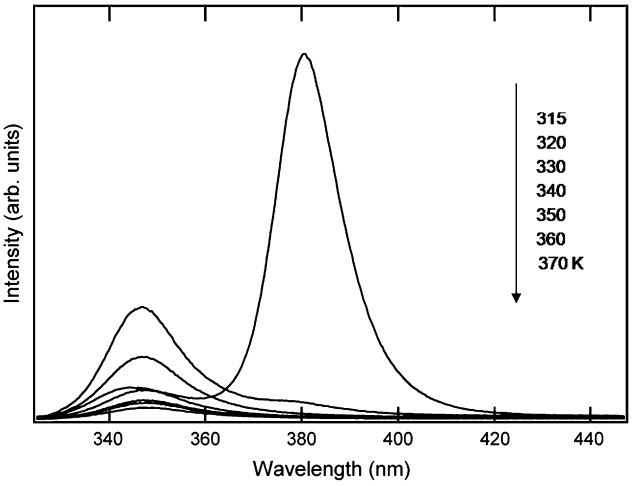


Fig. 5. Fluorescence spectra of the PDHS film in the temperature region from 315 to 370 K.

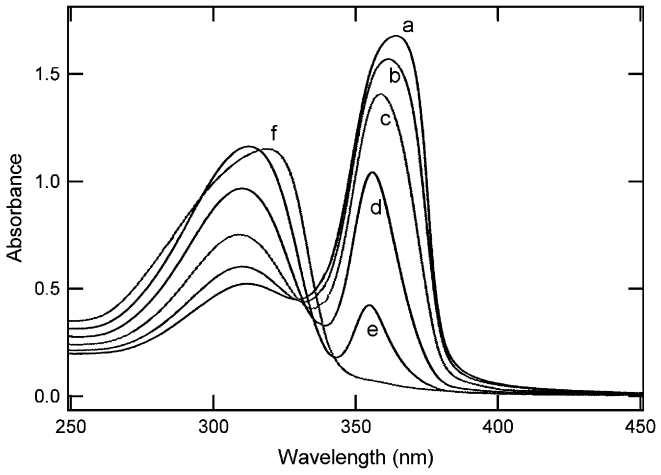


Fig. 6. Temperature dependence of the absorption spectrum of the PDHS film: (a) 293, (b) 303, (c) 308, (d) 311, (e) 313, (f) 315 K.

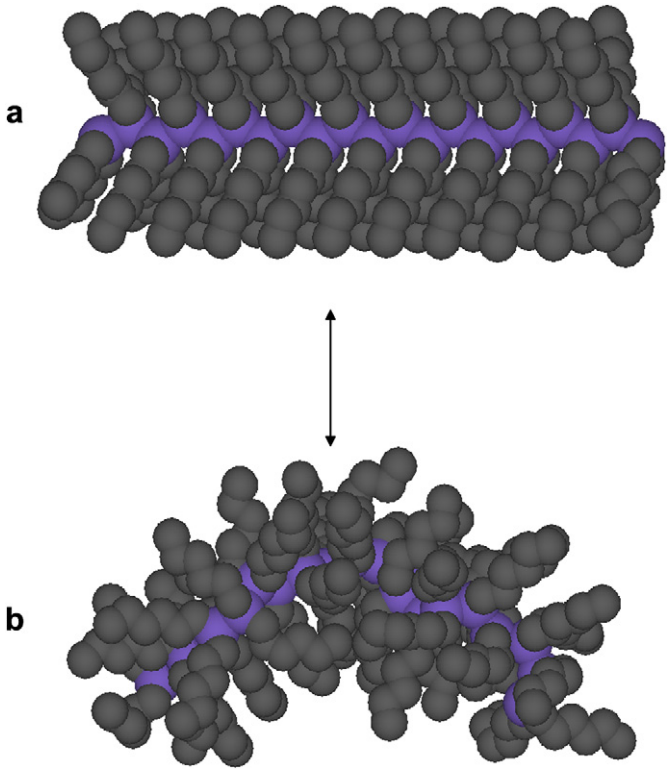


Fig. 7. The image of the order to disorder transition of the poly(di-*n*-hexylsilane). Molecular models of (a) all-*trans* conformation and (b) random coil conformation, where the hydrogen atoms are undisplayed because of the highlighting of the conformation of the Si–Si and C–C bonds.

conformations, respectively, where the hydrogen atoms are undisplayed because of the highlighting of the conformation of the Si–Si and C–C bonds. The σ-conjugation of the polysilane is quite sensitive to the conformation of the Si–Si main chain. Because the all-*trans* conformation has the most conjugated electronic state and the lowest band gap, the PDHS shows the fluorescence at the longest wavelength. With increasing the *gauche*-rich conformation, in other word, random coil structure, the σ-conjugation is reduced, which induces the increase of the band gap and the shift of the fluorescence peak to the shorter wavelengths.

### 3.3. DSC curves

DSC curves of the PDHS and PDHS/$TiO_2$ nanoparticle hybrid are shown in Fig. 8. The PDHS shows a sharp endothermic peak at 315 K. The temperature corresponds to the order–disorder transition temperature of the PDHS.

At the transition temperature, the melting of the *n*-hexyl side chain has been observed by wide-angle X-ray diffraction (WAXD) of the PDHS [2,3,5]. Above the side-chain melting temperature, the substituent groups become disordered and conformationally mobile, which induce the disordered structure of the Si–Si main chain. It has been reported that side-chain crystallization causes the ordering of the Si–Si main chain by IR and Raman studies [2,4,5]. This suggests that significant intermolecular interactions (i.e., side-chain crystallization) are necessary to drive the backbone into the all-*trans*

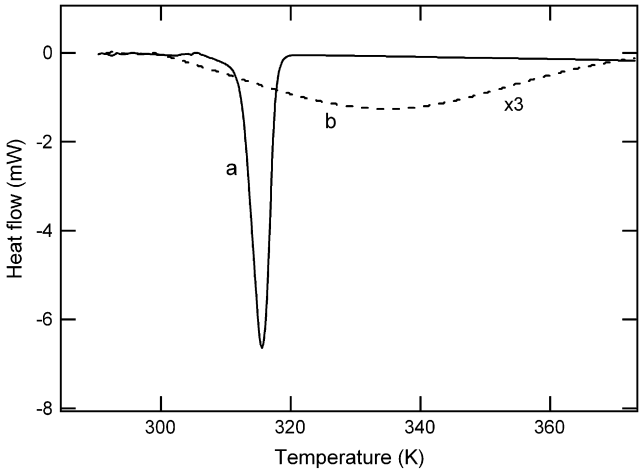


Fig. 8. DSC curve of (a) the PDHS and (b) the PDHS/$TiO_2$ nanoparticle hybrid film under He. Heating rate: 5 °C/min.

(planar zigzag) conformation for the sterically encumbered PDHS. The fluorescence peak shift of the ordered structure in the temperature region from 80 to 260 K (Fig. 3) may be related to the relaxation of the side chains. When the PDHS film was cooled from room temperature to 80 K in a cryostat before measurements, the turbulence of the polymer chain at room temperature is frozen in the glassy state at 80 K. The turbulence of the *n*-hexyl side chain perturbs the planar zigzag conformation of Si–Si main chain because the all-*trans* structure of the main chain needs the alignment and the packing of the *n*-hexyl side chain as shown in Fig. 7a. Therefore, the torsional angles of the Si–Si main chain have a distribution around the conformation with a minimum steric energy. The relaxation of the side chain is induced by the temperature rise in the low temperature region from 80 to 260 K, which thaws the frozen conformation of the PHDS. This causes the alignment and the packing of the *n*-hexyl side chain and the Si–Si main chain. The shift of the fluorescence peak to the longer wavelengths in the temperature region from 80 to 260 K (Fig. 3) can be attributed to the above structural change. As shown in Fig. 8b, the PDHS/$TiO_2$ nanoparticle hybrid shows rather broad DSC curve, which may be due to a distribution of the intermolecular interaction between the PDHS chain and the $TiO_2$ nanosurface. The $\Delta H$ value for the peaks of the PDHS and the PDHS/$TiO_2$ nanoparticle hybrid was −33 and −8 J/g, respectively.

### 3.4. Temperature dependence of the fluorescence of the PDHS/$TiO_2$ nanohybrid film

The temperature dependence of fluorescence of PDHS/$TiO_2$ nanoparticle hybrid film in the region from 80 to 160 K is shown in Fig. 9.

The 355-nm band of the PDHS/$TiO_2$ nanoparticle hybrid film at 80 K is an evidence of the interaction between the PDHS chain and the $TiO_2$ nanosurface. Such fluorescence similar to that of the *gauche*-rich structure must be caused by the disordering of the polymer chain at the boundary layer

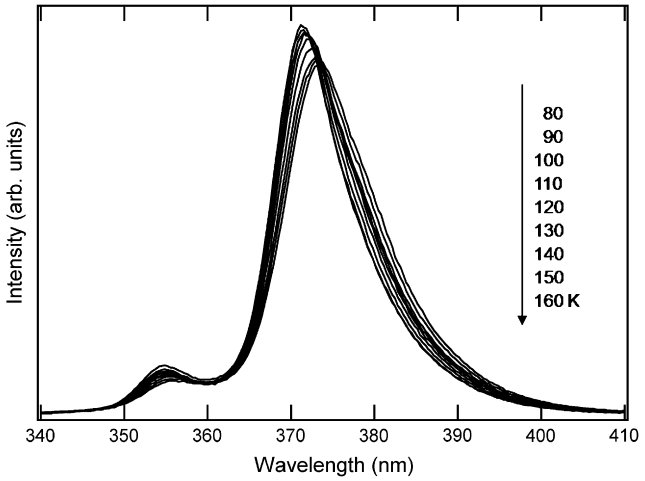


Fig. 9. Fluorescence spectra of the PDHS/$TiO_2$ nanoparticle hybrid film in the temperature region from 80 to 160 K.

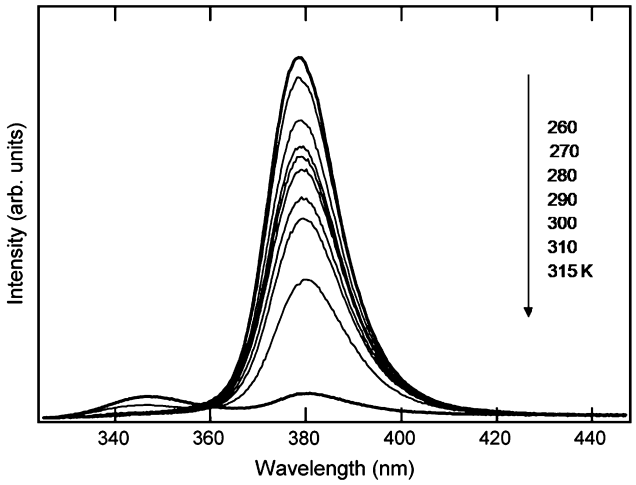


Fig. 11. Fluorescence spectra of the PDHS/$TiO_2$ nanoparticle hybrid film in the temperature region from 260 to 315 K.

between the PDHS and $TiO_2$ nanoparticle. In Fig. 9, the fluorescence spectra show the decrease of the intensity of the 355-nm band with increasing temperature. The intensity at around 370 nm also decreases with increasing temperature although the temperature dependence is not remarkable compared to the PDHS film. In the region from 160 to 260 K, the temperature dependence of the fluorescence intensity of the PDHS/$TiO_2$ nanoparticle hybrid film is quite different from that of the PDHS film. As shown in Fig. 10, the increase of the fluorescence intensity at around 375 nm was observed accompanying the decrease of the fluorescence intensity at 355 nm, where these fluorescences are originated from the ordered and disordered structures, respectively. After the disappearance of the 355-nm band, the fluorescence of the ordered structure exhibited a remarkable decrease in the temperature region from 260 to 315 K as shown in Fig. 11.

The order–disorder transition similar to the PDHS film is observed at around 315 K as shown in Fig. 12 although the DSC curve of the PDHS/$TiO_2$ nanoparticle hybrid is a broad

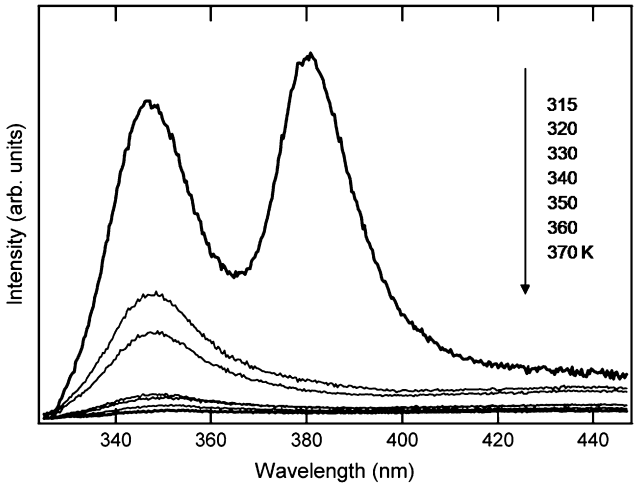


Fig. 12. Fluorescence spectra of the PDHS/$TiO_2$ nanoparticle hybrid film in the temperature region from 315 to 370 K.

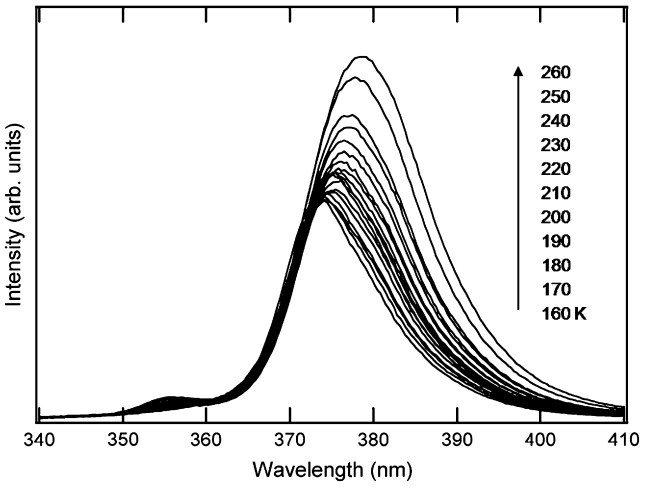


Fig. 10. Fluorescence spectra of the PDHS/$TiO_2$ nanoparticle hybrid film in the temperature region from 160 to 260 K.

one (Fig. 8b). When the ratio of the disorder band to the order band is compared between the PDHS (Fig. 5) and the PDHS/$TiO_2$ nanoparticle hybrid film (Fig. 12) at 315 K, the latter shows the higher ratio of the disorder band. This tendency is consistent with the DSC curve of the PDHS/$TiO_2$ nanoparticle hybrid film as shown in Fig. 8b, which shows the rise of the endothermic curve at the lower temperature than that for the PDHS film. This result also suggests the disordering of the polymer chain in the neighborhood of the $TiO_2$ nanosurface.

In the hybrid films, a new emission band appeared at the longer wavelength region than 420 nm with an increase in the temperature up to 320 K as shown in Fig. 12. The broad band can be assigned to the emission from a branching structure of the Si–Si chain. The branching Si–Si chain shows broad emission band at around 450 nm, which is induced by the photodecomposition of the Si–Si chain [25–28]. In the comparison of the PDHS and PDHS/$TiO_2$ nanoparticle hybrid films, the latter shows the broad emission band above 420 nm remarkably. This result is reasonably assigned to the

enhancement of the photodecomposition by the $TiO_2$ nanoparticle. The photodecomposition must be caused by the photoinduced electron transfer at the PDHS/$TiO_2$ nanoparticle heterojunction interface. The mixture of a conjugated polymer (p-type semiconductor) with $TiO_2$ (n-type semiconductor) leads to the formation of the bulk p–n heterojunction [19]. The photoinduced electron transfer between the PDHS and the $TiO_2$ nanoparticle is enhanced by the p–n heterojunction.

The temperature dependence of the fluorescence maximum wavelength of the ordered structure is compared between the PDHS and the PDHS/$TiO_2$ nanoparticle hybrid film in Fig. 13. The fluorescence maximum of the PDHS/$TiO_2$ film is observed at the shorter wavelength than that of the PDHS film, which suggests the perturbation of the polymer chain in the neighborhood of the $TiO_2$ nanosurface. Around the order–disorder transition temperature where the melting of the *n*-hexyl side chains occurs, the fluorescence maximum wavelengths of both films are almost similar. Therefore, the difference of the fluorescence maximum wavelength between the PDHS and the PDHS/$TiO_2$ nanoparticle hybrid films can be owing to the feature of the *n*-hexyl side chain in the neighborhood of the $TiO_2$ nanosurface.

Fig. 14 shows temperature dependence of the normalized fluorescence intensities of the PDHS and PDHS/$TiO_2$ nanoparticle hybrid films, where the intensities are normalized to those of the fluorescence maxima at 80 K. In the case of the PDHS/$TiO_2$ nanoparticle hybrid film, the fluorescence intensity of the 355-nm band assigned to the disordered structure decreases showing an inflection point at around 160 K. Contrary to the 355-nm band, the fluorescence intensity of the 380-nm band assigned to the ordered structure shows a turning point from decreasing to increasing at around 160 K in the region from 80 to 260 K. On the other hand in the range from 260 to 315 K, the fluorescence intensity of the ordered structure decreases accompanying the increase of that of the disordered structure. These results suggest that the disordered conformation in the Si–Si main chain acts as a quenching site. The excited state migrates along the Si–Si main chain after the excitation [29–35]. The excited state is trapped in some disorder-induced local potential minima. The non-radiative deactivation of the excited state occurs via the disorder-induced local potential minima. As shown in Fig. 12, the PDHS/$TiO_2$ hybrid film shows a new peak appeared at the longer wavelength region than 420 nm with an increase in the temperature up to 315 K, which can be assigned to the emission from a branching Si–Si chain generated by the photoinduced electron transfer at the p–n heterojunction interface between the PDHS and the $TiO_2$ nanoparticle. In the temperature region above around 315 K, the photoinduced electron transfer at the p–n heterojunction interface also lowers the fluorescence intensity.

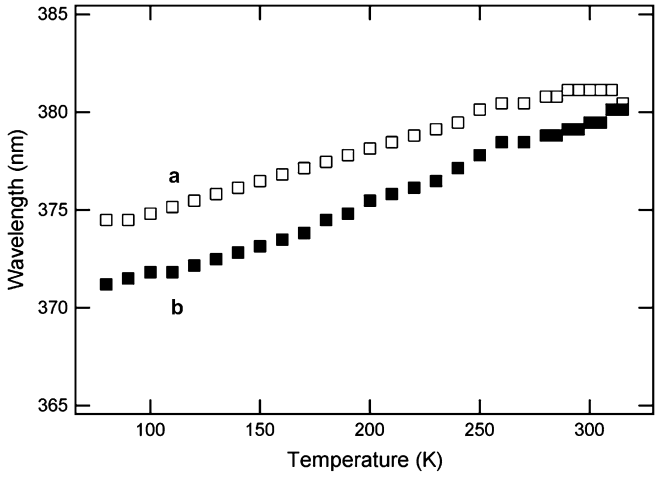


Fig. 13. Temperature dependence of the fluorescence maximum wavelength of (a) the PDHS and (b) the PDHS/$TiO_2$ nanoparticle hybrid films in the temperature region from 80 to 315 K.

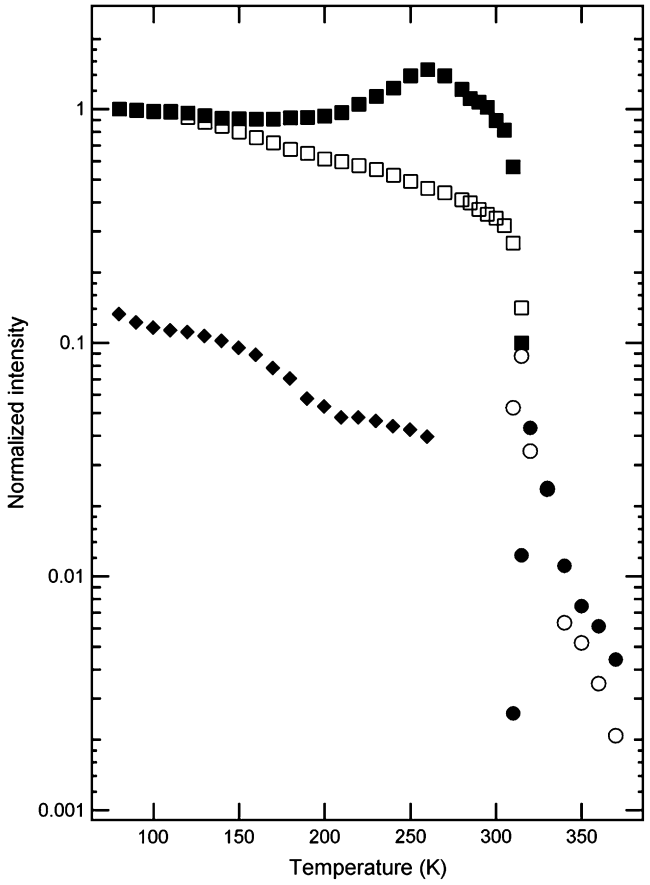


Fig. 14. Temperature dependence of the normalized fluorescence intensities of the PDHS and the PDHS/$TiO_2$ nanoparticle hybrid films. The intensities are normalized to those of the fluorescence maxima at 80 K. The plot shows the normalized fluorescence intensity for the PDHS film at around 380 (□) and 347 nm (○), and for the PDHS/$TiO_2$ nanoparticle hybrid film at around 380 (■), 355 (◆), and 347 nm (●).

The image of the PDHS chain around $TiO_2$ nanoparticle surface is illustrated schematically in Fig. 15. In the PDHS/$TiO_2$ nanoparticle hybrid film, a nanoporous structure must be formed by the aggregation of the $TiO_2$ nanoparticles. Some part of the PDHS chain is incorporated into the $TiO_2$ nanoporous structure. In the nanoporous structure, the conformation of the *n*-hexyl side chain is perturbed by the interaction between the side chain and the $TiO_2$ nanosurface. The perturbation of the *n*-hexyl side chain induces the disordered conformation of the Si–Si main chain. This must be the origin of the anomalous 355-nm band in the temperature region from 80 to

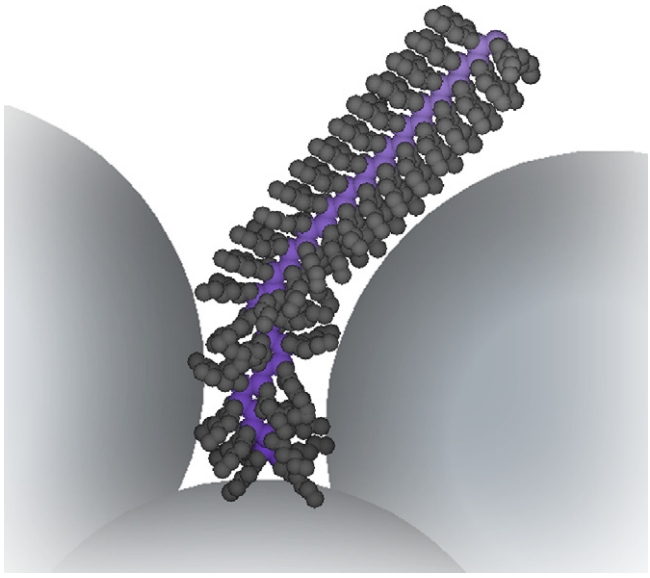

Fig. 15. The image of the poly(di-*n*-hexylsilane) chain in the neighborhood of the $TiO_2$ nanopore.

160 K. The influence of such a bound state may be reduced by thermal relaxation above 160 K.

## 4. Conclusion

The polysilane is a suitable probe to investigate the guest polymer–host matrix interaction because the photophysical properties of the polysilane remarkably depend on the conformation of the σ-conjugated Si–Si chain. We studied the fluorescence from PDHS/$TiO_2$ nanoparticle interface using PDHS as a probe to investigate the interaction between the polymer chain and the $TiO_2$ nanoparticle. The PDHS/$TiO_2$ nanoparticle hybrid film showed a fluorescence band assigned to a disordered structure even at 80 K, where the PDHS film showed only the fluorescence band of an ordered structure. The disordering of the polymer chain in the neighborhood of the $TiO_2$ nanosurface was suggested. Some part of the PDHS chain must be incorporated into the $TiO_2$ nanoporous structure which is formed by the aggregation of the $TiO_2$ nanoparticles. In the nanoporous structure, the conformation of the *n*-hexyl side chain is perturbed by the interaction between the side chain and the $TiO_2$ nanosurface, which causes the disordered conformation of the Si–Si main chain and the 355-nm band. The non-radiative deactivation of the excited state via the disorder-induced local potential minima was suggested by the temperature dependence of the fluorescence intensities of the disordered and ordered structures in the temperature region from 80 to 160 K.

## Acknowledgements

This work was partially supported by a Grant-in-Aid for Scientific Research (No. 17550183) from the Ministry of Education, Science and Culture of Japan, and by the Program Research, Center for Interdisciplinary Research, Tohoku University. This work was also supported in part by New Energy and Industrial Technology Development Organization (NEDO) of Japan.

## References

[1] Miller RD, Michl J. Chem Rev 1989;89:1359.
[2] Rabolt JF, Hofer D, Miller RD, Fickes GN. Macromolecules 1986; 19:611.
[3] Weber P, Guillon D, Skoulios A, Miller RD. J Phys Fr 1989;50:793.
[4] Bukalov SS, Teplitsky MV, Gordeev YY, Leites LA, Westb R. Russ Chem Bull Int Ed 2003;52:1066–77.
[5] Aihara S, Kamata N, Nishibori A, Nagumo K, Sato H, Terunuma D, et al. J Lumin 2000;87–89:745–7.
[6] Tachibana H, Matsumoto M, Tokura Y, Moritomi Y, Yamaguchi A, Koshihara S, et al. Phys Rev B 1993;47:4363.
[7] Nakamura T, Oka K, Naito H, Okuda M, Nakayama Y, Dohmaru T. Solid State Commun 1997;101:503–6.
[8] Xu Y, Fujino T, Watase S, Naito H, Oka K, Dohmaru T. J Appl Phys 1999;38:2609.
[9] Seki S, Kunimi Y, Nishida K, Yoshida Y, Tagawa S. J Phys Chem B 2001;105:900–4.
[10] Seki S, Matsui Y, Yoshida Y, Tagawa S, Koe JR, Fujiki M. J Phys Chem B 2002;106:6849–52.
[11] Sanji T, Takase K, Sakurai H. J Am Chem Soc 2001;123:12690–1.
[12] Sanji T, Nakatsuka Y, Sakurai H. Polym J 2005;37:1–6.
[13] Sanji T, Takase K, Sakurai H. Bull Chem Soc Jpn 2004;77:1607–11.
[14] Ostapenko N, Kozlova1 N, Suto S, Watanabe A. Fiz Nizk Temp 2006;32:1363–71.
[15] Ostapenko N, Telbiz G, Ilyin V, Suto S, Watanabe A. Chem Phys Lett 2004;383:456.
[16] Ostapenko N, Kotova N, Telbiz G, Suto S, Watanabe A. Fiz Nizk Temp 2004;30:658.
[17] Ostapenko N, Kotova N, Lukashenko V, Telbiz G, Gerda V, Suto S, et al. J Lumin 2005;112:381.
[18] Dementjev A, Gulbinas V, Valkunas L, Ostapenko N, Suto S, Watanabe A. J Phys Chem C 2007;111(12):4717–21.
[19] Watanabe A, Kasuya A. Thin Solid Films 2005;483:358–66.
[20] Ravirajan P, Haque SA, Durrant JR, Poplavskyy D, Bradley DDC, Nelson J. J Appl Phys 2004;95:1473.
[21] Slooff LH, Wienk MM, Kroon JM. Thin Solid Films 2004;451:634.
[22] Huisman CL, Goossens A, Schoonman J. Synth Met 2003;138:237.
[23] Onoda M, Tada K. Curr Appl Phys 2003;3:141.
[24] Grant CD, Schwartzberg AM, Smestad GP, Kowalik J, Tolbert LM, Zhang JZ. Synth Met 2003;132:197.
[25] Watanabe A, Miike H, Tsutsumi Y, Matsuda M. Macromolecules 1993; 26:2111–6.
[26] Fujiki M. Chem Phys Lett 1992;198:177.
[27] Watanabe A, Nanjo M, Sunaga T, Sekiguchi A. J Phys Chem A 2001; 26:6436–42.
[28] Watanabe A. J Organomet Chem 2003;685:122–33.
[29] Suto S, Suzuki H, Goto T, Watanabe A, Matsuda M. J Lumin 1996; 66–67:341–4.
[30] Suto S, Shimizu M, Goto T, Watanabe A, Matsuda M. J Lumin 1998; 76–77:486–90.
[31] Shimizu M, Suto S, Goto T, Watanabe A, Matsuda M. Phys Rev B 1998;58:5032–42.
[32] Shimizu M, Suto S, Yamamoto A, Goto T, Kasuya A, Watanabe A, et al. J Lumin 2000;87–89:933–5.
[33] Suto S, Ono R, Shimizu M, Goto T, Watanabe A, Fang MC, et al. J Lumin 2000;87–89:773–5.
[34] Shimizu M, Suto S, Yamamoto A, Kasuya A, Goto T, Watanabe A, et al. Phys Rev B 2001;64:115417-1–115417-9.
[35] Shimizu M, Ono R, Suto S, Goto T, Fang MC, Watanabe A, et al. J Lumin 2002;99:197–203.